Synthesis and Properties of [NiCp*(2,5-tBu$_2$PC$_4$H$_2$)], a 20-Valence-Electron Phosphanickelocene

Claire Burney,[b] Duncan Carmichael,*[a] Kareen Forissier,[a] Jennifer C. Green,*[b] François Mathey,[c] and Louis Ricard[a]

Dedicated to Dr. John M. Brown FRS on the occasion of his 65th birthday

Abstract: The reaction of the bulky phospholide salt Li(2,5-tBu$_2$PC$_4$H$_2$)·2THF (**1**; THF = tetrahydrofuran) with [NiCp*(acac)] (HCp* = pentamethylcyclopentadiene, Hacac = acetylacetone) gives the green air-sensitive phosphanickelocene [NiCp*(2,5-tBu$_2$PC$_4$H$_2$)] (**2**) in yields of about 85%. An X-ray structural determination of **2** shows long Ni–ring bonds and "delocalised" ring P–C and C–C bonds characteristic of a classical 20-valence-electron (ve) nickelocene. The electronic structure of **2** has been clarified through a combined Amsterdam density functional (ADF) and photoelectron spectroscopic study, which indicates that the higher lying semi-occupied molecular orbital (SOMO) (−5.82 eV) has a′ symmetry and that the phosphorus "lone pair" is energetically low-lying (−8.15 eV). Oxidation of phosphanickelocene **2** by $AgBF_4$ occurs quantitatively to give the corresponding air-sensitive orange phosphanickelocenium salt [NiCp*(2,5-tBu$_2$PC$_4$H$_2$)]-[BF_4] (**3**). This complex has also been characterised by an X-ray crystallographic study, which reveals long Ni–C_α and short C_α–C_β bonds in the phospholyl ligand indicative of a SOMO having a″ symmetry. PMe_3 reacts with **2** at room temperature to provoke a ring-slip reaction that gives the 18ve complex [NiCp*η^1-(2,5-tBu$_2$PC$_4$H$_2$)-(PMe_3)] (**4**), but shows no reaction with the phosphanickelocenium salt **3** under the same conditions.

Keywords: density functional calculations · metallocenes · nickel · phosphorus heterocycles · photoelectron spectroscopy

Introduction

In recent work, we have used sterically hindered phospholide anions to study the synthesis of phosphametallocenes containing the late transition metals.[1–3] The challenge in this area stems from the fact that incoming electrophiles tend to react initially at the phosphorus atom of the phospholide[4–6] so that, for soft metals, phosphido-bridged dimers[7] are often obtained in place of the desired η^5-sandwich complexes. These may be seen even in cases which appear particularly favourable to η^5-coordination, as exemplified in Equation (1).[8]

Phosphacobaltocenes and phosphanickelocenes are therefore difficult targets because the drive for the μ_2-mode might be expected to rise as the number of M-L antibonding electrons in the sandwich complexes increases from Fe to

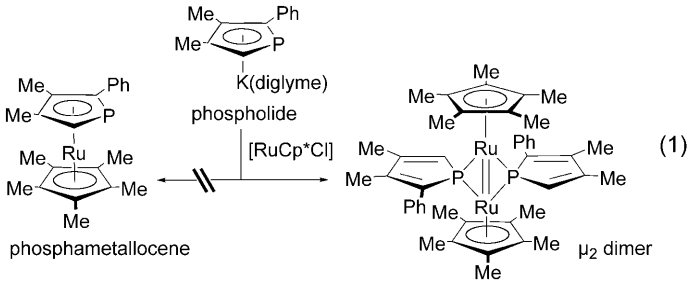

(1)

[a] Dr. D. Carmichael, Dr. K. Forissier, Dr. L. Ricard
Laboratoire Hétéroéléments et Coordination
UMR CNRS 7653, DCPH Ecole Polytechnique
91128 Palaiseau cedex (France)
Fax: (+33) 169-334-571
E-mail: duncan.carmichael@polytechnique.fr

[b] C. Burney, Prof. Dr. J. C. Green
Inorganic Chemistry Laboratory, University of Oxford
South Parks Rd, Oxford OX1 9QR (UK)
Fax: (+44) 1865-272-637
E-mail: jennifer.green@chem.ox.ac.uk

[c] Prof. Dr. F. Mathey
UCR–CNRS Joint Research Laboratory, University of California at Riverside, CA 92521 (USA)
Fax: (+1) 951 827 7850

 DOI: 10.1002/chem.200401293

Ni. We have recently had some success in using the 2,5-di-*tert*-butylphospholyl ligand **5**[1] to prepare a variety of unusual diamagnetic phosphametallocenes **6–8**[1,2] and the first stable monophosphacobaltocene **9**,[3] and were interested to employ the same ligand in an attempt to generate and understand an example of the still-unknown class of paramagnetic phosphanickelocenes.[9–11]

A number of previous studies could potentially have given rise to phosphanickelocenes. The earliest, employing heavily substituted di- and triphospholide anions, gave diamagnetic mononuclear 18ve ring-slipped sandwich complexes **10**[12] and **11**.[13] One of these was fluxional,[13] but neither showed paramagnetism. A related nickel η^3-triphosphacyclopentenyl complex was also prepared.[14] The study most closely resembling the work presented here involved the reaction of a tetramethylphospholide anion with [$NiCl_2$] which gave an 18ve bridged dimeric species **12**.[7] Finally, a much more recent study using triphospholide anions in reactions with [Ni(PPh_3)$_2$$Cl_2$] and [NiCl($PPh_3$)NO] gave 18ve monomers and dimers (Scheme 1) but no evidence for a 20ve species.[15,16]

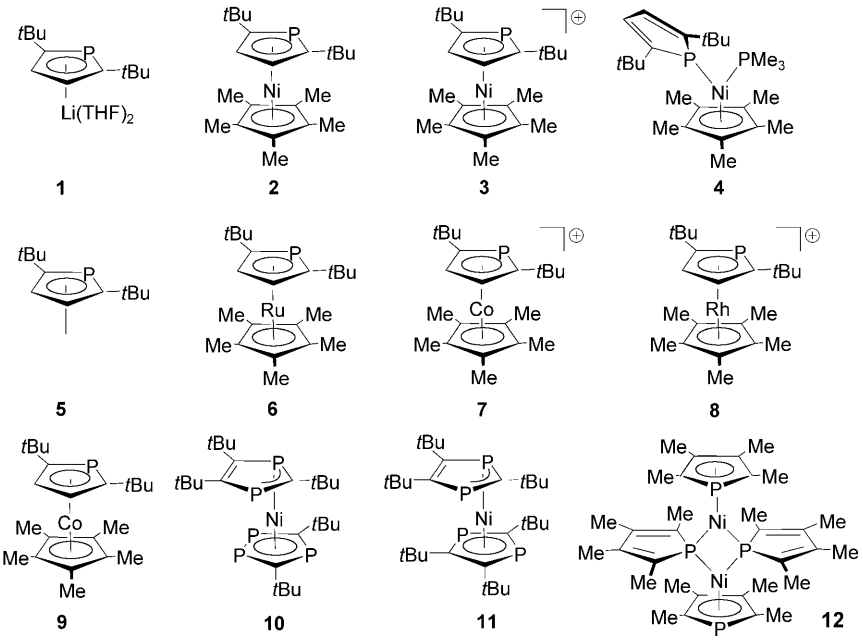

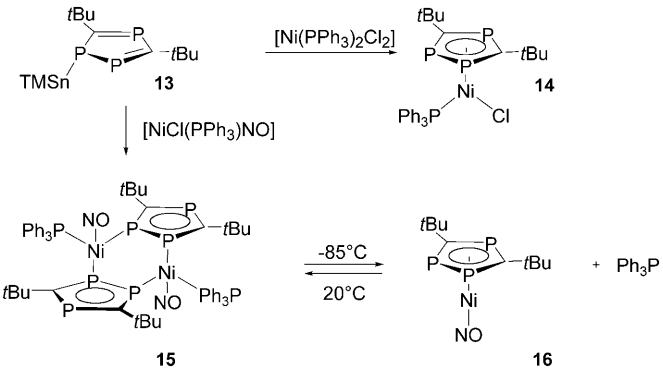

Scheme 1. Interaction of the triphospholide source **13** with Ni^{II} precursors.

Abstract in French: *La réaction du sel de phospholure encombré Li(2,5-tBu$_2$PC$_4$H$_2$)·2THF **1** (THF = tetrahydrofurane) avec [NiCp*(acac)] (HCp* = pentaméthylcyclopentadiène, Hacac = acetylacetone) fournit le phosphanickelocène [NiCp*(2,5-tBu$_2$PC$_4$H$_2$)] **2**, produit vert et sensible à l'air, avec un rendement de 85 %. La structure de **2** au rayons -X, qui met en évidence des liaisons Ni-cycle longues et les liaisons PC et CC délocalisées, est en bon accord avec une structure classique de métallocène à 20 électrons de valence (VE). D'après des études de spectroscopie photoélectronique (PES) et des calculs ADF (Amsterdam Density Functional), la combinaison nonliante du phosphore se trouve à −8.15 eV et la SOMO la plus haute, de symétrie a', est à −5.82 eV. Le phosphanickelocène **2** subit à une oxydation propre en présence de AgBF$_4$ pour fournir quantitativement le sel de phosphanickelocénium [NiCp*(2,5-tBu$_2$PC$_4$H$_2$)][BF$_4$] **3**, produit orange et sensible à l'air. La structure de **3** aux rayons-X met en évidence des liaisons Ni-C$_\alpha$ et C$_\alpha$-C$_\beta$ courtes, ce qui est en accord avec la SOMO de symétrie a'' qui est calculé par ADF. En réaction avec la triméthylphosphine, **2** subit un glissement de cycle pour donner le complexe à 18e [NiCp*η^1-(2,5-tBu$_2$PC$_4$H$_2$)(PMe$_3$)] **4**. Dans les mêmes conditions, le sel de phosphanickelocénium **3** reste inerte.*

The phosphanickelocene **2** and phosphanickelocenium salt **3** described here therefore constitute the first genuine 20- and 19ve sandwich complexes of phospholyl ligands at nickel centres.

Synthesis: Monophosphanickelocene **2** can be prepared in excellent yield by addition of the lithium phospholide Li(2,5-*t*Bu$_2$PC$_4$H$_2$)·2THF (**1**)[17,18] to [NiCp*(acac)][19,20] in THF at −78 °C [Eq. (2)]. After the mixture had been warmed to room temperature, an extraction into degassed pentane and purification by sublimation (40 °C, 1×10^{-2} mmHg), gave **2** as air-sensitive green needles in yields of about 85 %.

Complex **2** is stable in dry degassed pentane, toluene and dichloromethane and may be handled briefly (1–2 min) in air in the solid state. Electrochemical studies show a clean and reversible oxidation wave (+0.03 V in THF, SCE) and the phosphanickelocene undergoes a quantitative reaction

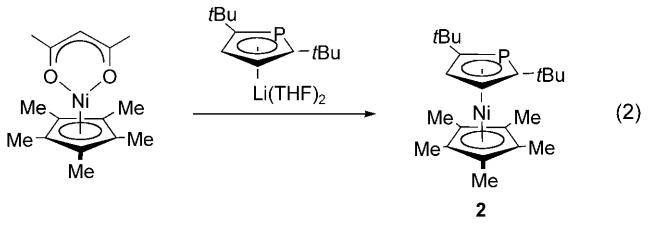

(2)

with silver tetrafluoroborate in dichloromethane to give, after removal of elemental silver, an air-sensitive solution of the phosphanickelocenium salt [NiCp*(2,5-tBu$_2$PC$_4$H$_2$)][BF$_4$] (**3**) [Eq. (3)]. The orange-gold complex **3** obtained after recrystallisation from chloroform–toluene is stable in degassed dichloromethane but is unstable over protracted periods in tetrahydrofuran.[21] It may be handled for short periods in air.

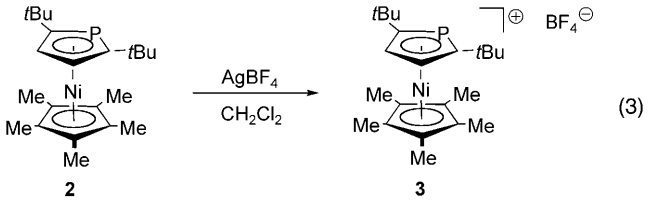

(3)

X-ray diffraction studies: Good quality monocrystals of phosphanickelocene **2** suitable for an X-ray diffraction study were obtained by reduced pressure (1.10^{-2} mmHg) sublimation at 40 °C and measured under a stream of cold nitrogen at 150 K. Refinement converged straightforwardly upon a classical sandwich complex where the eclipsed Cp* and phospholyl ligands straddle a mirror plane lying perpendicular to the phospholyl ligand and bisecting the P and Ni atoms (Figure 1, Table 1). Sites of residual electron density were found between the centroid-Ni-centroid axis and the C_β atoms on the side of the five-membered rings remote from the nickel atom. In total, they represented two electrons.

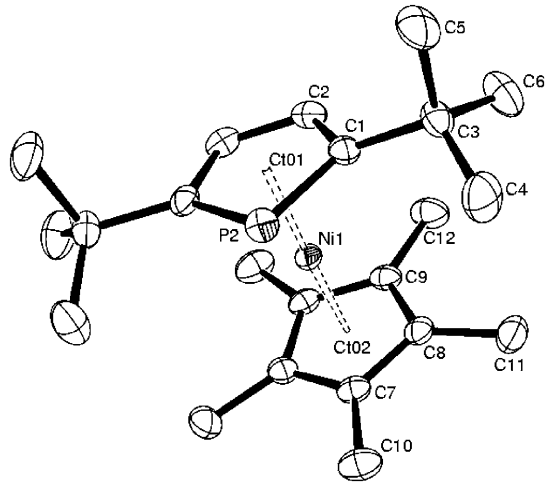

Figure 1. Molecular structure of phosphanickelocene **2**. Selected interatomic lengths [Å]: P2–C1 1.774(2), C1–C2 1.419(3), C2–C2′ 1.419(4), C7–C8 1.422(3), C8–C9 1.427(3), C9–C9′ 1.424(4). Primed and unprimed atoms are related by the molecular mirror plane.

Crystals of the phosphanickelocenium salt **3** were grown by diffusion of toluene into a chloroform solution of the complex and were also measured under cold nitrogen at 150 K (Figure 2, Table 1). As with the isoelectronic phosphacobaltocene,[3] the ligands are slightly staggered and the complex shows a C13-Ct1-Ct2-P1 dihedral angle of 17.7°. The shortest heavy atom contacts between the anion and the cation (both 3.06 Å) are from F4 to C15 and C16 and the influence of the anion appears to be reflected in an abnormally long P1–C4 bond (1.800(2) Å). Sites of residual electron density totalling one electron were found in similar zones to those in **2**.

For comparative purposes, the phosphaferrocene **17** was prepared by using classical chemistry [Eq. (4)], sublimed and also investigated crystallographically (150 K, Figure 3). It provides a useful benchmark for the class of [MCp*(2,5-tBu$_2$PC$_4$H$_2$)] structures, which also includes M = Co$^+$,[2] Rh$^+$,[2] Co[3] and Ru.[17]

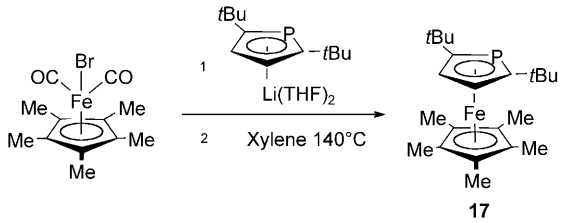

(4)

The phospholyl and pentamethylcyclopentadienyl ligands in the phosphanickelocene **2** display ring bond lengths and angles that are quite similar to those in the phosphaferrocene **17** (Figure 4). These confirm a broadly cylindrical electron density distribution about the centroid-Ni-centroid axis which is in sharp contrast with more localised bonding schemes found for the slipped di- and triphospholyl ligands in the 18ve nickel-containing complexes **10**[22] and **11**.[13] The major differences between the phosphaferrocene **17** and the phosphanickelocene **2** are found in the metal–ring distances. These are all longer in **2** but show a distinct trend, moving from M–C_β (7.3% longer in the Ni case) to M–C_α (6.1%) and M–P (4.2%) with values to the Cp* also being between 7.0 to 5.7% longer in **2**. The disproportionately small increase in the Ni–P bond length and preferential dissociation of the carbon atoms from the phosphametallocene with increasing electron count suggest the possibility of a soft potential surface for an η^5- to η^1- ring shift. This is investigated below.

Although the phosphanickelocenium structure **3** is perturbed by the presence of the anion, it shows a distinct shortening (by 1.5%) of the mean C_α–C_β and lengthening of the C_β–$C_{\beta'}$ and Ni–C_α separations (2.1 and 4.8% respectively) relative to the phosphaferrocene **17** (Figure 5). The Ni–C_α

Table 1. A summary of data pertaining to the crystal structures of complexes **2**, **3**, **4** and **17** and their refinement.[a]

Compound	**2**	**3**	**17**	**4**
M_r [Daltons]	389.16	475.99	386.32	465.25
space group	*Pnma*	$P2_1/c$	$P\bar{1}$	$P2_1/n$
a [Å]	11.4882(3)	13.431(5)	10.7778(4)	11.035(5)
b [Å]	17.7814(7)	10.089(5)	12.8962(3)	14.378(5)
c [Å]	10.5541(5)	17.431(5)	16.5175(5)	17.114(5)
α [°]	90	90	78.753(2)	90
β [°]	90	92.190(5)	79.230(1)	108.550(5)
γ [°]	90	90	70.839(2)	90
U [Å^{-3}]	2155.95(14)	2360.3(16)	2108.19(11)	2574.3(17)
Z	4	4	4	4
ρ_{calcd} [g cm^{-3}]	1.199	1.340	1.217	1.200
$F(000)$	840	1004	832	1008
μ [cm^{-1}]	0.975	0.927	0.792	0.886
h [°]	−16 to 15	−17 to 17	−15 to 15	−15 to 15
k [°]	−25 to 16	−10 to 13	−18 to 18	−18 to 20
l [°]	−14 to 14	22 to 22	−23 to 23	−24 to 23
size [mm]	0.18×0.12×0.08	0.20×0.16×0.04	0.18×0.18×0.18	0.32×0.24×0.08
independent refl	3238	5390	12202	7383
refined refl	2740	4158	9369	5961
wR_2 [$I>2\sigma(I)$]	0.1203	0.0837	0.0921	0.1005
R_1	0.0447	0.0326	0.0376	0.0336
GOF on F^2	1.019	1.030	1.047	1.090
max peak; min hole [eÅ^{-3}]	2.49(8); −0.55(8)	0.42(6); −0.36(6)	0.40(6); −0.45(6)	0.53(8) −0.36(8)

[a] All structures measured on collected on a Kappa CCD diffractometer using graphite-monochromated $Mo_{K\alpha}$ radiation of $\lambda=0.71070$ Å at 150 K. In all cases reflections with intensity $>2\sigma(I)$ were refined on F^2 using direct methods in SHELXL. CCDC-258269 (**2**), CCDC-258270 (**3**), CCDC-258271 (**17**), CCDC-258272 (**4**) contain the supplementary crystallographic data for this paper. These data can be obtained free of charge from The Cambridge Crystallographic Data Centre via www.ccdc.cam.ac.uk/data_request/cif.

lengthening, the effects are more pronounced in the phosphanickelocenium case.

Nuclear magnetic resonance measurements: Complexes **2** and **3** give distinctive solution ^{1}H NMR spectra[24] that exhibit the classical arrangement of high-field CH and low-field *t*Bu and Cp* protons which typify alicyclic nickelocene and nickelocenium salts,[24,25] as a result of positive ligand spin density at the ring carbon atoms. For the phosphanickelocene **2**, both the CH and CMe shifts lie slightly downfield from their analogues in [NiCp$_2$] and [NiCp$_2^*$];[26] these downfield shifts are also in agreement with DFT results which show greater mean spin density on the Cp* ring carbon atoms than those of the phospholyl ligand CH carbon atoms in **2** (see Table 2).

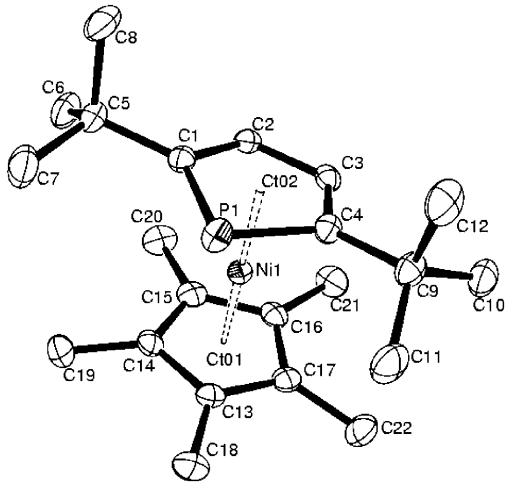

Figure 2. Molecular structure of phosphanickelocenium salt **3**. Selected bond lengths [Å]: P1–C1 1.786(2), P1–C4 1.800(2), C1–C2 1.400(2), C2–C3 1.443(2), C3–C4 1.390(2), C13–C14 1.454(2), C14–C15 1.410(3), C15–C16 1.447(3), C16–C17 1.415(2), C17–C13 1.429(2).

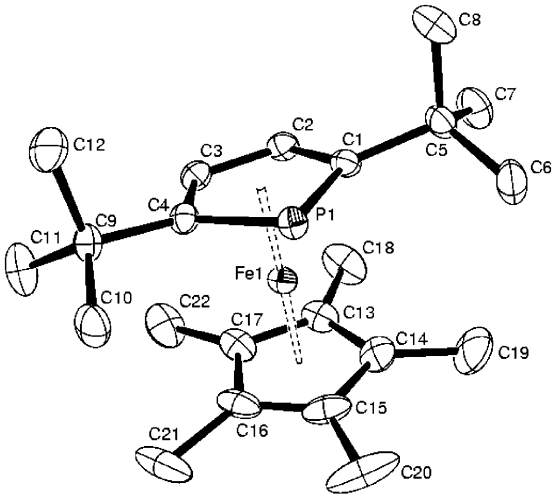

Figure 3. Molecular structure of one of the two crystallographically distinct molecules found in the unit cell of phosphaferrocene **17**. Mean selected interatomic lengths [Å]: P1–C1 1.785(2), C1–C2 1.417(2), C2–C3 1.411(2), C13–C17 1.423(2), C13–C14 1.427(2), C14–C15 1.424(3).

bonds also lengthen disproportionately (+4.8%) relative to Ni–P and Ni–C_β (+2.0 and +2.8%, respectively). These data unambiguously identify the a″ symmetric orbital (π_{as}, Figure 6) as the principal phospholyl component of the SOMO.[23] Similar changes are found in the isoelectronic phosphacobaltocene **9**[3] but, except for the degree of C_β–$C_{\beta'}$

The phosphanickelocenium salt **3** shows Cp* proton chemical shifts close to those found in the related nickelocenium salts[24] but a numerically small value for the CH proton shifts. As with the corresponding phosphacobaltocene **9**, this reflects the relatively small spin density at the phospholyl β carbon atoms.[3] The broad upfield-shifted ^{31}P

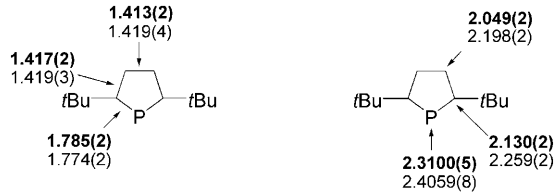

Figure 4. A comparison of bond lengths (Å) for the phospholyl ligand in [NiCp*(2,5-tBu$_2$PC$_4$H$_2$)] (**2**; normal text) and [FeCp*(2,5-tBu$_2$PC$_4$H$_2$)] (**17**; bold; mean values from the two crystallographically distinct molecules). Left: intracyclic separations, right: distances to the metal.

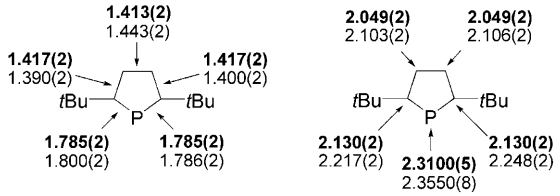

Figure 5. A comparison of bond lengths (Å) for the phospholyl ligand in [NiCp*(2,5-PC$_4$$tBu_2H_2$)][BPh$_4$] (**3**; normal text) and [FeCp*(2,5-PC$_4$$tBu_2H_2$)] (**17**; bold; mean values from the two crystallographically distinct molecules). Left: intracyclic separations, right: distances to the metal.

Figure 6. Phospholyl π-symmetric combinations.

Table 2. Paramagnetic shifts for selected sandwich phosphametallocenes [MCp*(2,5-tBu$_2$PC$_4$H$_2$)] quoted relative to phosphaferrocene **17** (cations as BF$_4$ salts). ^{1}H NMR data for Cp*, CH and tBu protons and ^{31}P data for phosphorus.

	C*H*	Cp*	*t*Bu	P	solvent
Co$^+$[2] (**7**)	−0.5	−0.6	0.1	−63	$CDCl_3$
Fe (**17**)	0	0	0	0	C_6D_6
Co[3] (**9**)	20.3	−40.6	−5.5	47	C_6D_6
Ni$^+$ (**3**)	52.8	−110.9	−11.6	121	CD_2Cl_2
Ni (**2**)	184.7	−261.2	−14.4		C_6D_6

resonance (−190 ppm, $\nu_{1/2}$ 350 Hz) found in the phosphanickelocenium salt **3** implies a small and negative electron spin density at phosphorus[3] and is consistent with the a″-symmetric SOMO found in the gas-phase calculations for **3**. The formal reduction of **3** to **2** populates the a′-symmetric orbital and places significant unpaired spin density on the phosphorus. Consistently, no ^{31}P resonance could be detected for **2** between ±3000 ppm.

Photoelectron spectroscopy: The He I and He II photoelectron (PE) spectra of [NiCp*(2,5-tBu$_2$PC$_4$H$_2$)] (**2**) are shown in Figure 7 and ionisation energies (IEs) are given in Table 3. The spectra are consistent with a genuine metallocene formulation and the low-energy region, bands A–C, strongly resembles those found in [NiCp$_2^*$] and [NiCp$_2$].[27] The first two ionisations are little separated and appear at essentially the same energy as the degenerate e_{1g} pair in [NiCp$_2^*$]. The remaining bands are in accord with earlier work but the multiplicity and overlapping nature of ionisations between 7–9 eV means that, except for the phosphorus-derived bands, the individual components can only be ordered precisely by numerical calculation (below).

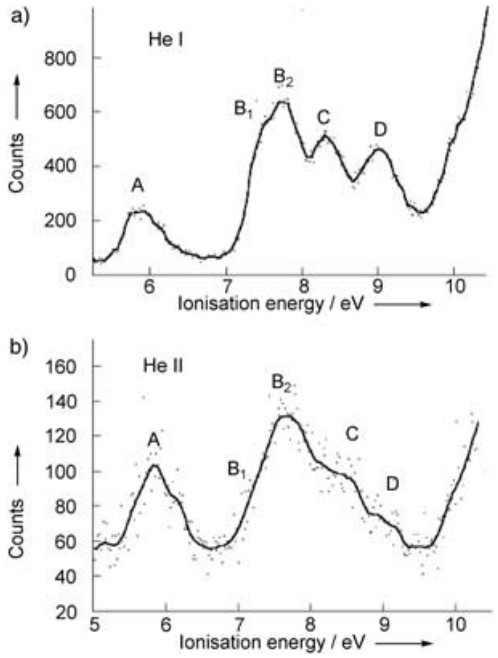

Figure 7. He I and He II PE spectra for [NiCp*(2,5-tBu$_2$PC$_4$H$_2$)] **2**.

Table 3. Calculated and experimental IE for [NiCp*(2,5-tBu$_2$PC$_4$H$_2$)] (**2**), comparison with those of [NiCp$_2$] and [NiCp$_2^*$], and assignments of the metallocene bands.

Orbital	MCp$_2$ analogue	IE$_{calcd}$ [eV] α Spin	β Spin	IE$_{exptl}$ [eV] **2**	[NiCp$_2^*$]	MCp$_2$ assignment
42a′	e_{1g}*	5.65	–	5.82 (A)	5.82	$^2E_{1g}$
32a″	e_{1g}*	5.80	–			
31a″	e_{1u}	7.40	7.10	7.39 (B$_1$)	7.47	$^4E_{1u}$, $^2E_{1u}$
41a′	e_{1u}	7.41	7.18			
40a′	e_{2g}	7.74	7.42	7.67 (B$_2$)	7.71	$^4A_{2g}$, $^4E_{2g}$
30a″	e_{2g}	7.97	7.58			
39a′	a_{1g}	7.99	7.64			
38a′	Pσ	8.33	7.97	8.24 (C)	8.40	$^2A_{2g}$, $^4E_{1g}$, $^2E_{2g}$
29a″	e_{1g}	8.78	8.11			
37a′	e_{1g}	9.02	8.52	8.94 (D)	8.50	$^2E_{1g}$

Band D, at 8.94 eV, is more intense in the PE spectrum of **2** than in that of [NiCp$_2^*$]. It also shows diminished relative intensity in the He II spectrum, as does band C. Such characteristics are consistent with ion states associated with the phosphorus atom of the phospholyl ring. These ionisations are very similar to those of the corresponding phosphacobaltocene **9** (8.24, 8.89 eV)[3] and are markedly easier to effect than those in simple organic compounds containing sp^2-hy-

bridised phosphorus centres such as phosphinines,[28–30] phosphaalkynes[31,32] or phosphaalkenes,[33,34] and other phosphametallocenes.[35–37] However, they remain high with respect to classical phosphines[38] so that the phosphorus centre must be characterised as weakly basic.

Density functional calculations: Geometry optimisations were performed for **2**, **3** and **17** with spin states 1, 1/2 and 0, respectively. C_s symmetry was assumed. Little energy difference was found between structures with a staggered or eclipsed conformation of the rings and the results for a staggered conformation are reported. Figure 8 compares the experimental with the calculated distances. The results are in good agreement with the X-ray data; in particular, the series trends outlined above are reproduced by the DFT calculations. The geometry of [NiCp*(2,5-tBu$_2$PC$_4$H$_2$)] was also optimised with a spin state of 0. This was found to lie 0.42 eV higher in energy than the triplet state consistent with the paramagnetic state observed experimentally for **2**.

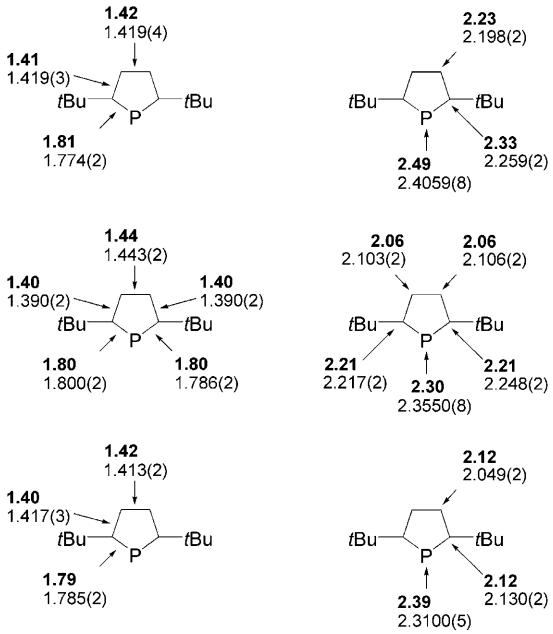

Figure 8. A comparison of experimental (normal text) and calculated (bold) bond lengths concerning the phospholyl ligand (2,5-tBu$_2$PC$_4$H$_2$) in **2** (top), **3** (middle) and **17** (bottom). Left: intracyclic separations, right: distances to the metal (Å).

Key orbitals are shown as isosurfaces in Figure 9. The two half-occupied orbitals of **2,** 42a′ and 32a″, resemble strongly the e_{1g} orbitals of nickelocene and are metal ligand antibonding. Their occupancy is the cause of the longer Ni–P and Ni–C bond lengths found for **2** compared with **17** where they are unoccupied. The higher lying SOMO 42a′ is of a′ character. It shows strong localisation on the phosphorus atom. The calculated energy gap to the lower-lying SOMO 32a″, which has a node at phosphorus is 0.16 eV, in accord with the quasidegeneracy of the PE ionisations. For **3** only

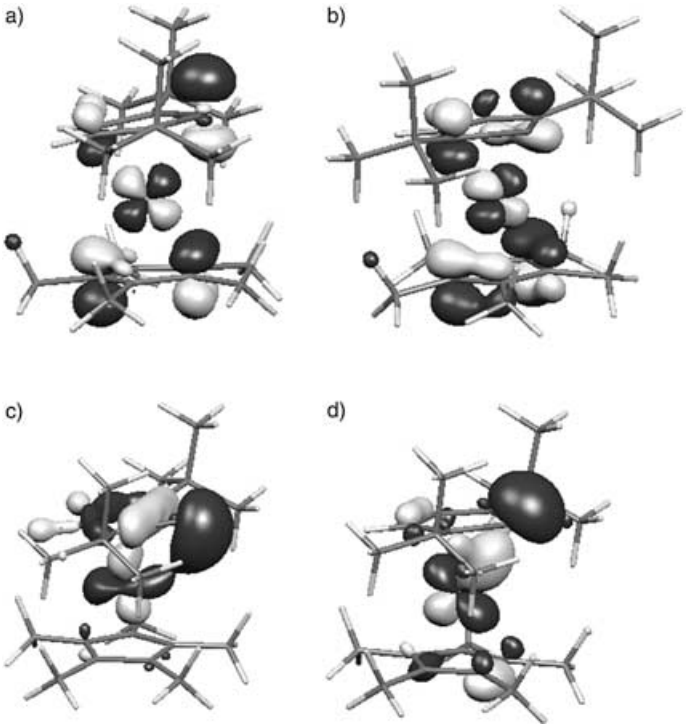

Figure 9. ADF-calculated isosurfaces for the SOMOs a) 42a′ and b) 32a″ and principal phosphorus-containing orbitals c) 38a′ and d) 37a′ in **2**.

32a″ is half-occupied. The shortening of C_α–C_β and lengthening of the C_β–$C_{\beta'}$ compared with **17** is consistent with the nodal properties of 32a″. Also the node at P accounts for the small change in M–P distance between **17** and **3**, whereas the half-filling of 42a′ results in a significant increase in Ni–P bond length in **2**.

Calculated spin densities for **2** and **3** are shown in Table 4. The P has a large positive spin density in **2** as a consequence of the population of 42a′ and a small negative spin density in **3** as inferred from the NMR studies. In both cases the spin density on the Cp* ring carbon atoms is greater than that on the phospholyl ligands, and that on the phospholyl β carbon atoms of **3** is the smallest.

Table 4. Calculated spin densities on atoms in **2** and **3.**

Atom	**2**	**3**
Ni	1.003	0.428
P	0.131	−0.025
C_α	0.068	0.106
C_β	0.074	0.026
Cp* C	0.112, 0.117, 0.111	0.134, 0.029, −0.028

The calculated IEs are given in Table 3 and have been used to assign the PE bands. Agreement between the calculated and experimental values is very good for the first band that is assigned to the two high-lying half-occupied orbitals 42a′ and 32a″.

Band A shows the greatest intensity increase in the HeII spectrum. This is generally the case with metallocene e_{1g}

ionisations and may be attributed to a shape resonance.[39] Band B_1 is assigned to ionisations from orbitals 31a′ and 41a′, the equivalent of the e_{1u} orbitals of [$NiCp_2^*$]. The metal bands associated with orbitals 39a″, 30a″ and 40a′ contribute to band B_2 which shows an intensity increase with increasing photon energy attributable to Ni 3d character in the associated orbitals. Band C arises from orbitals 38a′ and 29a″ and band D from 37a′. The surfaces in Figure 9 show that 38a′ has P ring σ character, whereas 37a′ shows the phosphoyl ring π orbital bonding with a Ni d orbital.

A calculation on the PC_4H_4 anion has the energy ordering P ring π > C ring π > P σ. Thus, the ordering of the derived orbitals is reversed upon complexation. The π orbitals are stabilised by bonding to the Ni and the 37a′ α spin orbital experiences further exchange stabilisation.

The metal e_{1g} orbitals show little change in IE upon passing from the phosphacobaltocene to the phosphanickelocene but the e_{2g} and a_{1g} orbitals show the sharp rise in IE typically found in [MCp_2] complexes. The "metallocene" formulation of **2** is therefore clearly confirmed.

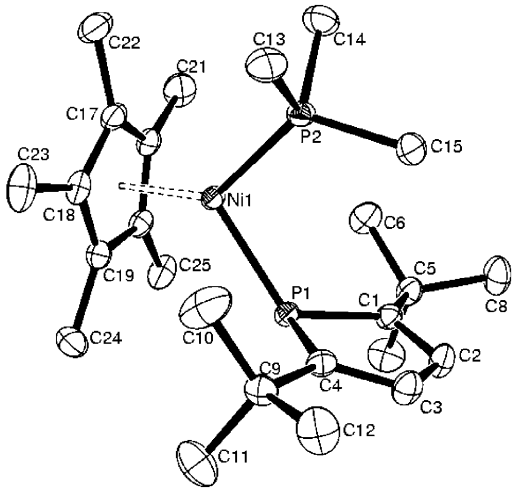

Figure 10. Molecular structure of adduct **4**. Selected interatomic lengths [Å] and angles [°]: Ni–P1 2.2195(7), Ni1–P2 2.1412(6), P1–C4 1.806(2), P1–C1 1.799(2), C1–C2 1.365(2), C2–C3 1.426(2), C3–C4 1.369(2); P1-Ni1-P2 98.41(2).

Chemical stability; reaction with trimethylphosphine: Given the existence of products **10**–**12**,[7,12,13] and the stronger calculated binding of sp^2 phosphorus than carbon to the metal centre in some phosphametallocenes,[40,41] it seems likely that the energy barrier for ring slippage reactions of the phospholyl ligands at nickel may be relatively small. Furthermore, the spatial accessibility of the lone pairs in unhindered phosphanickelocenes and phosphanickelocenium salts will probably drive the ring-slip process. Thus, to provide a broad approximation of the interaction of unhindered phosphanickelocene derivatives with themselves, **2** and **3** were allowed to react with trimethylphosphine.[42] The phosphanickelocenium salt **3** proved inert even upon stirring at room temperature with excess trimethylphosphine over several days. However, reaction between **2** and PMe_3 occurred instantaneously and quantitatively in dichloromethane at 25 °C to give an air-stable deep purple diamagnetic complex which was shown to be **4** by X-ray diffraction [Eq. (5)].

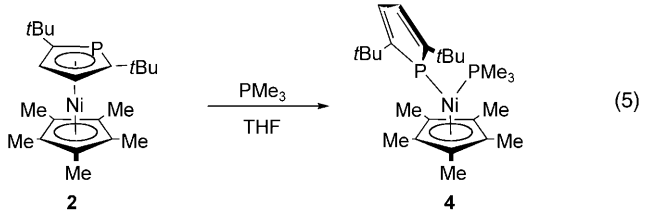

(5)

No further reaction was observed with excess PMe_3. Complex **4** gives a mass spectrum base peak corresponding to [M^+–PMe_3], but gentle heating under a dynamic vacuum gave no evidence for the liberation of trimethylphosphine or the regeneration of **2**.

The X-ray structure of **4** (Figure 10) shows the near-planar phospholyl ring anticipated for η^1-ligated phospholyl metal complexes[22,43] and a lesser degree of C–C bond length alternation than the bridged dimer **12**,[7] thus suggesting some residual phospholyl aromaticity and charge separation in the complex. The structure shows strong indications of steric crowding. The most significant of these are the perfect intercalation of the C15 atom between the phospholyl *tert*-butyl groups and the fold angle of 20.5° made between the mid-point of the C2–C3 bond with the P1 and Ni1 atoms. This ensures that the phosphorus lone pair is oriented towards the Cp* ligand in a position poorly adapted to further coordination.

In the light of the existence of dimer **12** and the chemistry above, a final series of experiments was undertaken to investigate the interaction of the relatively unhindered phospholide salt K(3,4-$Me_2PC_4H_2$)[44] with [NiCp*(acac)] [Eq. (6)]. Reaction at −78 °C in THF gave an intense purple-red diamagnetic solution that, upon extraction with pentane and crystallisation, gave a deep purple microcrystalline powder. The high-field ^{31}P NMR shift and mass spectrum showing a peak corresponding to the molecular ion [NiCp*(3,4-$Me_2PC_4H_2$)]$_2^+$ indicate the formation of an Arliguie/Ephritikhine-type[7] dimer **18**, so it is improbable that the presence of the Cp* ligand in **2** (as opposed to the two phospholyls in Ephritikhine's case) suffices in itself to explain the stability of the monomeric form.

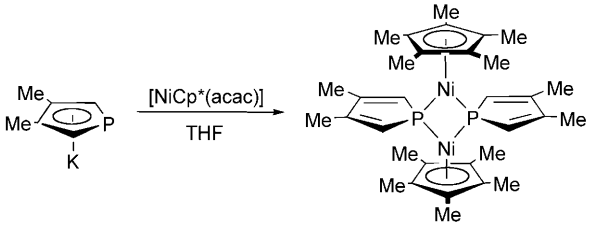

(6)

To investigate the energetics of the dimerisation further by means of theoretical calculation we compared the energy of the sterically unencumbered monomer, $[Ni(\eta\text{-}PC_4H_4)_2]$ (**19**) with the dimer $[\{Ni(\eta\text{-}PC_4H_4)(\mu\text{-}PC_4H_4)\}_2]$ (**20**). The SCF energy for the dimer was found to be 140 kJ mol^{-1} more stable than two monomers, a clear indication that the metallocene-like monomer **2** would be stabilised by the steric bulk of the ring substituents.

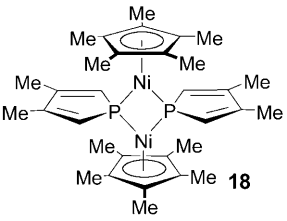

18

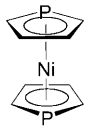

19

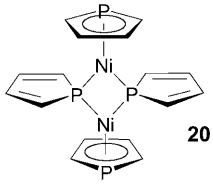

20

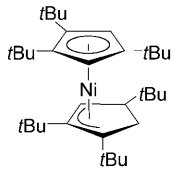

21

Discussion

This study provides the first demonstration that, under appropriate conditions, phosphanickelocenes and phosphanickelocenium salts can exist as stable entities. These results are in accord with the high aromaticity associated with the phospholide anion[45–48] and underline its similarities with cyclopentadienides.[49] The inherent stability of the 19ve phosphanickelocenium sandwich configuration is not entirely clear at this stage because of the absence of useful phosphorus-containing reference structures. Nonetheless, it seems evident that the 20ve (phosphanickelocene) configuration becomes unstable with respect to other structures as the hindrance about the phosphorus atom decreases or as the number of phosphorus atoms within the phospholyl rings increases.

The role of hindrance seems to be reasonably clear-cut. For monophospholyl ligands, no clear evidence for ring slippage from the η^5- to η^3-coordination mode has appeared to date.[50] However, both in Ephritikhine's[7] and our work it has been possible to observe 18 ve nickel-containing structures that are formally the products of an η^5- to η^1-ring shift occurring in a phosphanickelocene structure.[51–53] The X-ray data suggesting that the carbon atoms preferentially peel away from the metal centre upon moving from phosphaferrocene **17** to phosphanickelocene **2**, and the DFT results showing the high electron density at the phosphorus atom of **2**, seem to indicate that the preferred structure for a simple unencumbered "monophosphanickelocene" will be a dimer such as **18**. The 20ve configuration will become stable when the hindrance in the coordination sphere rises sufficiently to prevent the phospholyl ligand from adopting an orientation favourable to bridging: a situation that clearly exists in the structure found for **4**. The factors determining the structural changes upon passing from **2** to **10** and **11** are less obvious. 1,1′,2,2′,4,4′-hexa(*tert*-butyl)nickelocene is unknown and the cocondensation of nickel atoms with 1,2,4-tri(*tert*-butyl)cyclopentadiene gives the η^3-cyclopentenyl nickel complex **21**[54] so it is possible that the 18ve structure observed in **11**[13] may reflect steric issues.[55] However, the hindrance in complex **10**[12] is rotationally quite nicely equilibrated and in this case the multiple *t*Bu substitution alone seems unlikely to impose a ring-slipped 18ve configuration. The difference in the electronic structure can be more reasonably attributed to the lowered HOMO–LUMO gap in the polyphospholyl ligand and the consequent increase in its ligand field strength.[40,56,57]

A number of other simple phosphametallocene redox pairs[3,58,59] are known but the phosphanickelocene–phosphanickelocenium couple described here provides an interesting case where significant electron spin can be switched on to or away from the phosphorus atom by redox chemistry at the directly bound nickel centre. Research aimed at clarifying the implications of this effect is in progress.

Experimental Section

General: All operations were performed either by using cannula techniques on Schlenk lines under an atmosphere of dry nitrogen or in a Braun Labmaster 130 drybox under dry purified argon. Hydrated $[Ni(acac)_2]$ was dried by azeotropic distillation with toluene[60] and Li(2,5-*t*Bu$_2$PC$_4$H$_2$)·2THF (**1**) was prepared as described previously.[1,18] THF and $[D_6]$benzene were distilled from sodium-benzophenone ketyl and pentane from sodium-benzophenone ketyl-tetraglyme under an atmosphere of dry nitrogen and stored over activated 4 Å molecular sieves prior to use. Chloroform and dichloromethane were distilled from P_4O_{10} under nitrogen and also stored for short periods over 4 Å molecular sieves. The electrochemical measurement is referenced to SCE and was made on a Digital DEA-1 apparatus at platinum electrodes under dry argon in THF using a 0.3 M *n*Bu$_4$NBF$_4$ electrolyte. NMR measurements were made on a Bruker AM 200 spectrometer and are referenced to internal C_6D_5H or C_4D_7HO and external H_3PO_4. Mass spectra were obtained under 70 eV electron impact by using direct inlet methods on a Hewlett Packard 5989B spectrometer. HeI (21.22 eV) and HeII (40.81 eV) photoelectron spectra were recorded by using a PES laboratories Ltd 0078 spectrometer interfaced to an Atari microprocessor. They were calibrated by using He, Xe and N_2.

Theoretical methods: Calculations were performed by using density functional methods of the Amsterdam Density Functional Package (version 2000.02).[61,62] Type IV basis sets were used with triple ξ accuracy sets of Slater type orbitals, with a single polarisation function added to the main group atoms. The cores of the atoms were frozen up to 2p for Ni, 1 s for C and 2p for P. The generalised gradient approximation (GGA nonlocal) method was used, using Vosko, Wilk and Nusair's local exchange correlation[63] with non-local exchange corrections by Becke,[64] non local correlation corrections by Perdew.[65] Ionisation energies were calculated by direct calculations on the molecular ions in their ground and appropriate excited states and subtraction of the energy of the neutral molecule.

Pentamethylcyclopentadienyl-2,5-di(*tert*-butyl)phospholylnickel(II) (2): A solution of $[Ni(acac)_2]$ (0.500 g, 1.95 mmol) in dry and degassed THF (25 mL) was cooled to −78 °C and treated dropwise with a THF (15 mL)

suspension of LiCp* (0.277 g, 1.95 mmol) which had been precooled to −78 °C. The solution was warmed slowly to −10 °C and, after stirring until red, recooled to −78 °C and further treated with a solution of Li(2,5-*t*Bu$_2$PC$_4$H$_2$)·2 THF (0.710 g, 1.95 mmol) in THF (20 mL) at −78 °C. After slow warming to room temperature, the green mixture was evaporated to dryness, extracted into pentane (30 mL) and filtered through celite. Further evaporation to dryness followed by sublimation (70 °C, 0.01 mmHg) gave green air- and moisture-sensitive single crystals of **2** (0.660 g, 87 %). ^{1}H NMR (200 MHz, [D$_6$]benzene): δ = 263.0 (s, $\nu_{1/2}$ = 1060 Hz; Cp*), 15.7 (s, $\nu_{1/2}$ = 140 Hz; *t*Bu), −180.3 ppm (s, $\nu_{1/2}$ = 1200 Hz; CH); μ_{eff}[66,67] = 2.78 BM ([D$_6$]benzene 298 K); MS (70 eV): *m/z* (%): 388 (100), [*M*$^+$], 331 (64) [*M*$^+$−C$_4$H$_9$], 316 (98) [*M*$^+$−C$_5$H$_{12}$].

Pentamethylcyclopentadienyl-2,5-di(*tert*-butyl)phospholylnickel(III) tetrafluoroborate (3): Phosphanickelocene **2** (0.100 g, 0.26 mmol) was dissolved in dry degassed dichloromethane (15 mL) and the solution was treated at room temperature with solid silver tetrafluoroborate (0.028 g, 0.26 mmol). The orange-red solution was stirred for 15 min, filtered through a celite pad to remove deposited elemental silver and evaporated to dryness. Recrystallisation from $CHCl_3$/toluene gave orange air-sensitive needles of [NiCp*(2,5-*t*Bu$_2$PC$_4$H$_2$)][BF$_4$] (**3**; 0.90 g, 74 %). ^{1}H NMR (200 MHz, CD_2Cl_2): δ = 112.7 (s, $\nu_{1/2}$ = 1340 Hz; Cp*), 12.9 (s, $\nu_{1/2}$ = 120 Hz; *t*Bu), −48.4 ppm (s, $\nu_{1/2}$ = 560 Hz; CH); ^{31}P NMR (80 MHz, [D$_6$]benzene): δ = −190.2 ppm (s, $\nu_{1/2}$ = 350 Hz).

Pentamethylcyclopentadienyl-2,5-di(*tert*-butyl)phospholyliron(II) (17): [Cp*Fe(CO)$_2$Br] (0.58 g, 1.76 mmol) and Li(2,5-*t*Bu$_2$PC$_4$H$_2$)·2 THF (**1**; 0.63 g, 1.82 mmol) were stirred in THF (20 mL) for 30 min. The orange-red solution was evaporated to dryness, extracted into dry degassed xylene (100 ml) and refluxed under a stream of nitrogen for 3 h. After filtration through celite and evaporation to dryness in vacuo, the product was purified by sublimation (130 °C, 0.01 mmHg). Slightly air-sensitive orange single crystals of **17** (0.37 g, 54 %) were collected and stored under nitrogen. ^{1}H NMR (200 MHz, [D$_6$]benzene): δ = 4.35 (d, ^3J(P,H) = 4.6 Hz; H3), 1.79 (s, Cp*), 1.30 ppm (s, *t*Bu); ^{13}C NMR (50 MHz, [D$_6$]benzene): δ = 117.3 (d, ^{1}J(P,C) = 61.3 Hz; C2), 82.4 (s; *C*Me), 79.4 (d, ^2J(P,C) = 4.8 Hz; C3), 34.3 (d, ^2J(P,C) = 14.0 Hz; *C*Me$_3$), 33.9 (d, ^3J(P,C) = 7.3 Hz; C*Me$_3$*), 13.1 ppm (s, C*Me*); ^{31}P NMR (80 MHz, [D$_6$]benzene): δ = −79.3 ppm; MS (70 eV): *m/z* (%): 386 (100) [*M*$^+$], 329 (15) [*M*$^+$−C$_4$H$_9$], 314 (45) [*M*$^+$−C$_5$H$_{11}$].

Pentamethylcyclopentadienyl{η^1-2,5-di(*tert*-butyl)phospholyl}trimethylphosphinenickel(II) (4): A solution of **2** (0.100 g, 0.26 mmol) in dichloromethane (20 mL) was treated with trimethylphosphine (ca. 0.05 g, excess) at room temperature. After stirring for 20 min, the mixture was concentrated to about 1 mL and allowed to crystallise. Deep purple air-sensitive crystals of **4** (0.113 g, 95 %) were collected and dried in vacuo. X-ray quality crystals were grown from pentane by slow evaporation of the solvent. ^{1}H NMR (200 MHz, [D$_6$]benzene): δ = 7.14 (dd, ^2J(P,H) = 10.2, ^3J(P,H) = 2.1 Hz; H3), 1.63 (dd, ^3J(P,H) = 2.0, 0.5 Hz; Cp*), 1.61 ppm (d, ^3J(P,H) = 0.4 Hz; *t*Bu); ^{13}C NMR (50 MHz, [D$_6$]benzene):δ = 170.6 (dd, ^1J(P,C) = 16.1, ^3J(P,C) = 3.8 Hz; C2), 125.5 (d, ^2J(P,C) = 9.7 Hz; C3), 102.7 (s; *C*Me), 36.3 (d, ^2J(P,C) = 13.3 Hz; *C*Me$_3$), 35.8 (d, ^{3}J(P,C) = 5.9 Hz; C*Me$_3$*), 14.9 (d, ^1J(P,C) = 28.7 Hz; P*Me*), 11.3 ppm (d, ^3J(P,C) = 4.0 Hz; C*Me*); ^{31}P NMR (80 MHz, [D$_6$]benzene): δ = −7.8 (s), −9.8 ppm (s); MS (70 eV): *m/z* (%): 388 (100) [*M*$^+$−PMe$_3$], 331 (63) [*M*$^+$−PMe$_3$$^+$−C$_4H_9$], 316 (88) [*M*$^+$−PMe$_3$$^+$−C$_5H_{11}$].

Bis(pentamethylcyclopentadienyl)-bis-μ$_2$-(3,4-dimethylphospholyl)dinickel(II) (18): A −78 °C solution of [Ni(acac)$_2$] (0.196 g, 0.76 mmol) in dry and degassed THF (50 mL) was treated dropwise with a THF (15 mL) suspension of LiCp* (0.108 g, 0.76 mmol), which was precooled to −78 °C. After warming slowly to 0 °C, the deep red solution was recooled to −78 °C and treated with a solution of K(3,4-Me$_2$PC$_4$H$_2$) (0.200 g, 0.76 mmol) in THF (20 mL) at −78 °C. After slow warming to room temperature, the deep purple mixture was evaporated to dryness, extracted into pentane and filtered through celite. Concentration gave purple essentially air-stable microcrystals of **18** (0.28 g, 67 %). ^{31}P NMR (80 MHz, [H$_8$]THF): δ = −129 ppm. MS (70 eV): *m/z* (%): 608 (12), [*M*$^+$], 304 (100) [(*M*/2)$^+$].

Acknowledgements

We thank CNRS, Ecole Polytechnique (studentship to K.F.), EPSRC, Somerville College Oxford, and the Oxford Supercomputing centre for support, and Dr. P. Le Floch for some technical assistance in obtaining the voltammogram.

[1] D. Carmichael, L. Ricard, F. Mathey, *J. Chem. Soc. Chem. Commun.* **1994**, 1167.
[2] K. Forissier, L. Ricard, D. Carmichael, F. Mathey, *Organometallics* **2000**, *19*, 954.
[3] C. Burney, D. Carmichael, K. Forissier, J. C. Green, F. Mathey, L. Ricard, *Chem. Eur. J.* **2003**, *9*, 2567.
[4] L. S. Sunderlin, D. Panu, D. B. Puranik, A. J. Ashe, III, R. R. Squires, *Organometallics* **1994**, *13*, 4732.
[5] F. Mathey, *Coord. Chem. Rev.* **1994**, *137*, 1.
[6] E. H. Braye, I. Caplier, R. Saussez, *Tetrahedron* **1971**, *27*, 5523.
[7] T. Arliguie, M. Ephritikhine, M. Lance, M. Nierlich, *J. Organomet. Chem.* **1996**, *524*, 293.
[8] D. Carmichael, F. Mathey, L. Ricard, N. Seeboth, *Chem. Commun.* **2002**, 2976.
[9] D. Carmichael, F. Mathey, *Top. Curr. Chem.* **2002**, *220*, 27.
[10] C. Burney, D. Carmichael, K. Forissier, J. C. Green, F. Mathey, L. Ricard, S. Wendicke, *Phosphorus Sulfur Silicon Relat. Elem.* **2002**, *177*, 1999.
[11] N. Kuhn, G. Henkel, J. Kreutzberg, S. Stubenrauch, C. Janiak, *J. Organomet. Chem.* **1993**, *456*, 97.
[12] R. Bartsch, P. B. Hitchcock, J. F. Nixon, *J. Organomet. Chem.* **1989**, *373*, C17.
[13] F. G. N. Cloke, K. R. Flower, C. Jones, R. M. Matos, J. F. Nixon, *J. Organomet. Chem.* **1995**, *487*, C21.
[14] V. Caliman, P. B. Hitchcock, J. F. Nixon, *Chem. Commun.* **1997**, 1739.
[15] F. W. Heinemann, H. Pritzkow, M. Zeller, U. Zenneck, *Organometallics* **2000**, *19*, 4283.
[16] J. Heinicke, N. Gupta, S. Singh, A. Surana, O. Kuhl, R. K. Bansal, K. Karaghiosoff, M. Vogt, *Z. Anorg. Allg. Chem.* **2002**, *628*, 2869.
[17] D. Carmichael, L. Ricard, F. Mathey, *J. Chem. Soc. Chem. Commun.* **1994**, 2459.
[18] E. J. M. de Boer, I. J. Gilmore, F. M. Korndorffer, A. D. Horton, A. van der Linden, B. W. Royan, B. J. Ruisch, L. Schoon, R. W. Shaw, *J. Mol. Catal.* **1994**, *90*, 171.
[19] E. E. Bunel, L. Valle, J. M. Manriquez, *Organometallics* **1985**, *4*, 1680.
[20] M. E. Smith, R. A. Andersen, *J. Am. Chem. Soc.* **1996**, *118*, 11119.
[21] P. Lemoine, M. Gross, P. Braunstein, F. Mathey, B. Deschamps, J. H. Nelson, *Organometallics* **1984**, *3*, 1303.
[22] R. Bartsch, D. Carmichael, P. B. Hitchcock, M. F. Meidine, J. F. Nixon, G. J. D. Sillett, *J. Chem. Soc. Chem. Commun.* **1988**, 1615.
[23] D. L. Dubois, C. W. Eigenbrot, A. Miedaner, J. C. Smart, R. C. Haltiwanger, *Organometallics* **1986**, *5*, 1405.
[24] J. Blümel, N. Hebendanz, P. Hudeczek, F. H. Köhler, W. Strauss, *J. Am. Chem. Soc.* **1992**, *114*, 4223.
[25] F. H. Köhler, K. H. Doll, W. Prössdorf, *J. Organomet. Chem.* **1982**, *224*, 341.
[26] U. Kölle, F. Khouzami, *Angew. Chem.* **1980**, *92*, 658; *Angew. Chem. Int. Ed. Engl.* **1980**, *19*, 640.
[27] C. Cauletti, J. C. Green, M. R. Kelly, P. Powell, J. Van Tilborg, J. Robbins, J. Smart, *J. Electron Spectrosc. Relat. Phenom.* **1980**, *19*, 327.
[28] C. Batich, Heilbron. E, V. Hornung, A. J. Ashe, D. T. Clark, U. T. Cobley, D. Kilcast, I. Scanlan, *J. Am. Chem. Soc.* **1973**, *95*, 928.
[29] L. Nyulászi, G. Keglevich, *Heteroat. Chem.* **1994**, *5*, 131.
[30] A. Schweig, W. Schafer, K. Dimroth, *Angew. Chem.* **1972**, *84*, 636; *Angew. Chem. Int. Ed. Engl.* **1972**, *11*, 631.
[31] J. C. T. R. Burckett St-Laurent, P. B. Hitchcock, M. A. King, H. W. Kroto, M. F. Meidine, S. I. Klein, S. I. Al Resayes, R. J. Suffolk, J. F. Nixon, *Phosphorus Sulfur Silicon* **1983**, *18*, 259.

[32] J. C. T. R. Burckett St-Laurent, M. A. King, H. W. Kroto, J. F. Nixon, R. J. Suffolk, *J. Chem. Soc. Dalton Trans.* **1983**, 755.
[33] S. Lacombe, D. Gonbeau, J. L. Cabioch, B. Pellerin, J. M. Denis, G. Pfister-Guillouzo, *J. Am. Chem. Soc.* **1988**, *110*, 6964.
[34] P. v. R. Schleyer, D. Kost, *J. Am. Chem. Soc.* **1988**, *110*, 2105.
[35] C. Guimon, G. Pfister-Guillouzo, F. Mathey, *Nouv. J. Chim.* **1979**, *3*, 725.
[36] C. Guimon, D. Gonbeau, G. Pfister- Guillouzo, G. de Lauzon, F. Mathey, *Chem. Phys. Lett.* **1984**, *104*, 560.
[37] D. Gonbeau, G. Pfister-Guillouzo, A. Marinetti, F. Mathey, *Inorg. Chem.* **1985**, *24*, 4133.
[38] P. B. Dias, M. E. M. Depiedade, J. A. M. Simoes, *Coord. Chem. Rev.* **1994**, *135*, 737.
[39] J. Brennan, G. Cooper, J. C. Green, M. P. Payne, C. M. Redfern, *J. Electron Spectrosc. Relat. Phenom.* **1993**, *66*, 101.
[40] J. Frunzke, M. Lein, G. Frenking, *Organometallics* **2002**, *21*, 3351.
[41] E. J. P. Malar, *Eur. J. Inorg. Chem.* **2004**, 2723.
[42] Analogous behaviour was seen with dmpe, PPh_3 and the electronically more representative $P(OMe)_3$.
[43] F. Mercier, L. Ricard, F. Mathey, *Organometallics* **1993**, *12*, 98.
[44] D. Baudry, F. Nief, in *Synthetic Methods of Organometallic and Inorganic Chemistry, (Herrmann/Brauer)*, *Vol. 9* (Ed.: W. A. Herrmann), Thieme, Stuttgart, **2000**.
[45] L. Nyulászi, *Chem. Rev.* **2001**, *101*, 1229.
[46] B. Goldfuss, P. von R. Schleyer, F. Hampel, *Organometallics* **1996**, *15*, 1755.
[47] D. B. Chesnut, L. D. Quin, *J. Am. Chem. Soc.* **1994**, *116*, 9638.
[48] E. J. P. Malar, *J. Org. Chem.* **1992**, *57*, 3694.
[49] K. B. M. Dillon, F. Mathey, J. F. Nixon, *Phosphorus, the carbon copy*, Wiley, Chichester, **1998**.
[50] It is, however, possible that substitution reactions at [Co(phospholyl)L_2] complexes follow a classical associative pathway which would imply a reversible high-energy substitution-driven η^5- to η^3-ring shift: A. J. M. Caffyn, D. Carmichael, F. Mathey, L. Ricard, *Organometallics* **1997**, *16*, 2049.
[51] T. K. Hollis, Y. J. Ahn, F. S. Tham, *Chem. Commun.* **2002**, 2996.
[52] T. K. Hollis, Y. J. Ahn, F. S. Tham, *Organometallics* **2003**, *22*, 1432.
[53] T. K. Hollis, L. S. Wang, F. S. Tham, *J. Am. Chem. Soc.* **2000**, *122*, 11737.
[54] J. J. Schneider, C. Kruger, *Chem. Ber.* **1992**, *125*, 843.
[55] R. Bartsch, F. G. N. Cloke, J. C. Green, R. M. Matos, J. F. Nixon, R. J. Suffolk, J. L. Suter, D. W. Wilson, *J. Chem. Soc. Dalton Trans.* **2001**, 1013.
[56] F. G. N. Cloke, J. C. Green, J. R. Hanks, J. F. Nixon, J. L. Suter, *J. Chem. Soc. Dalton Trans.* **2000**, 3534.
[57] G. Frison, F. Mathey, A. Sevin, *J. Phys. Chem. B* **2002**, *106*, 5653.
[58] R. Feher, F. H. Köhler, F. Nief, L. Ricard, S. Rossmayer, *Organometallics* **1997**, *16*, 4606.
[59] X. Sava, L. Ricard, F. Mathey, P. Le Floch, *Inorg. Chim. Acta* **2003**, *350*, 182.
[60] R. A. Schunn, S. D. Ittel, M. A. Cushing, *Inorg. Synth.* **1990**, *28*, 94.
[61] E. J. Baerends, A. Berces, C. Bo, P. M. Boerringter, L. Cavallo, L. Deng, R. M. Dickson, D. E. Ellis, L. Fan, T. H. Fischer, C. Fonseca Guerra, S. J. van Gisbergen, J. A. Groeneveld, O. V. Gritsenko, F. E. Harris, P. van den Hoek, H. Jacobsen, G. van Kessel, F. Kootstra, E. van Lenthe, V. P. Osinga, P. H. T. Philipsen, D. Post, C. C. Pye, W. Ravenek, P. Ros, P. R. T. Schipper, G. Schreckenbach, J. G. Snijiders, M. Sola, D. Swerhone, G. te Velde, P. Vernooijis, L. Versluis, O. Visser, E. van Wezenbeek, G. Wiesenekker, S. K. Wolff, T. K. Woo, T. Ziegler, *"ADF Program System Release 1999"*.
[62] C. Fonseca Guerra, J. G. Snijider, G. te Velde, E. J. Baerends, *Theor. Chem. Acc.* **1998**, *99*, 391.
[63] S. H. Vosko, L. Wilk, M. Nusair, *Can. J. Phys.* **1990**, *58*, 1200.
[64] A. D. Becke, *Phys. Rev* **1988**, *A38*, 2398.
[65] J. Perdew, *Phys. Rev. B* **1986**, *33*, 8822.
[66] D. F. Evans, *J. Chem. Soc.* **1959**, 2003.
[67] J. L. Deutsch, S. M. Poling, *J. Chem. Educ.* **1969**, *46*, 167.

Received: December 16, 2004
Revised: April 22, 2005
Published online: July 8, 2005